Chapter Three

Experimental Setup

3.1 : Introduction

The purpose of this experiment is to study an array of arc discharge for nitrogen laser. A laser channel has been constructed with 64 isolated cathodes at one side. This will allow the laser to discharge transversely. A 40 kV charger has been assembled as the power supply for the laser system. A ' C-to-C' discharge circuit has been employed to pulse the laser. A spark gap is used as the switching device. A vacuum pump has been used to provide the vacuum for this laser system. Nitrogen gas is pumped out from one outlet while new nitrogen gas will be pumped into the laser channel through another gas inlet. A valve is used to control the gas flow rate. Figure 3.1 shows the schematic drawing of the new transverse arc array discharge circuit design.

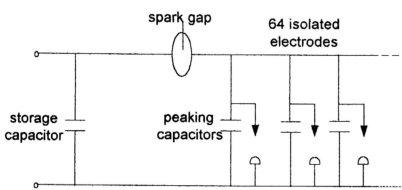

Figure 3.1 : Drawing of the transverse arc array discharge.

3.2 : Experimental Setup

A 22" x 45" aluminum plate has been used as the base for the whole system. This aluminum plate also acts as the ground plate for the discharge circuit. 64 doorknob capacitors are screwed onto this base plate. These doorknob capacitors act as the peaking capacitors for the 'C-to-C' circuit.

Various designs have been tried out to obtain the lowest inductance of the discharge circuit. Finally, it comes out with the design as shown in Fig. 3.2. The laser channel is put at one side of the plate while the storage capacitors are put at the other end of the plate.

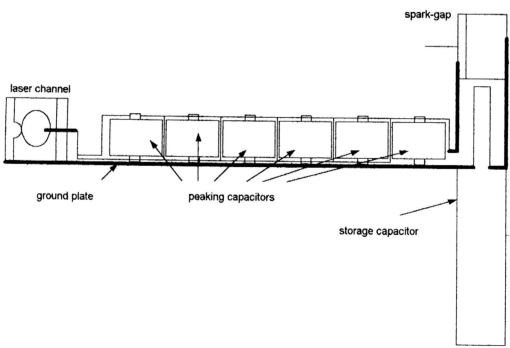

Figure 3.3 : The cross section view of the experimental setup.

All the wires are placed as close to the plate as possible. This will reduce the total cross section of the discharge loop to reduce the inductance of the circuit. Thus faster discharge will be obtained. Each door-knob peaking capacitor corresponds to one of the separated electrodes at the discharge channel and is connected by wires. In other words, the discharge of each electrode is independent from the others. All the wires are kept close to the ground plate as shown in Figure 3.3. The peaking capacitors are commonly charged up but discharged separately.

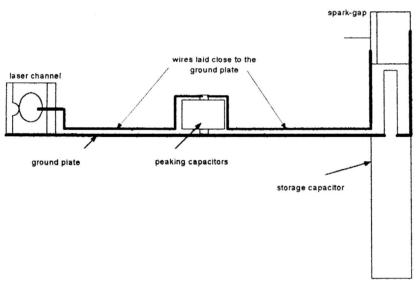

Figure 3.3 : The schematic drawing shows the setup and connection of one of the peaking capacitors and the storage capacitor. All wires are laid close to the ground plate.

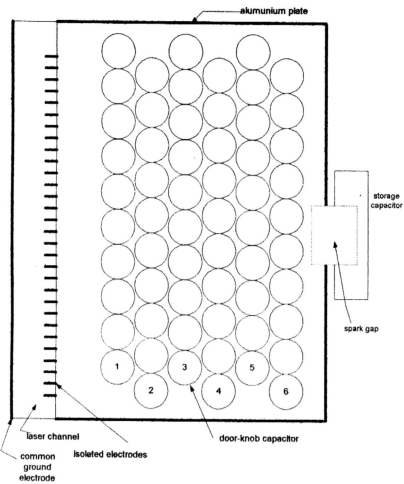

Figure 3.4 : Top view of the setup and the arrangement of peaking capacitors.

Since the objective of this project is to study this new discharge circuit, all the 64 electrodes are isolated. The arrangement of these 64 peaking capacitors will determine the charging and discharge time of the peaking capacitors. The discharge time of each electrode in the laser channel has to be synchronized for the laser to lase. The arrangement of the peaking capacitors is shown in Figure 3.4. The peaking capacitors are arranged in such a way that the first row (nearest to the laser channel)

may be charged up slightly slower than the sixth row (further away from the laser channel but nearest to the spark gap) but the time they discharge into the laser channel will be slightly faster and vice versa. Thus, every electrode will fire almost simultaneously.

3.3 : Design of laser channel

A 45" long laser channel has been constructed. The cathode and anode of the discharge are separated with perspex. The ground side of the laser channel is a brass plate with gas inlet and outlet. The assembly of these three components forms a laser channel.

Serious considerations have been made in order to isolate each electrode and also to be able to achieve good vacuum for the laser channel. A 45" x 2.5"x 0.3" nylon plate with 64 holes at the center of the plate to house the 64 electrodes are made as shown in Figure 3.5 has been made.

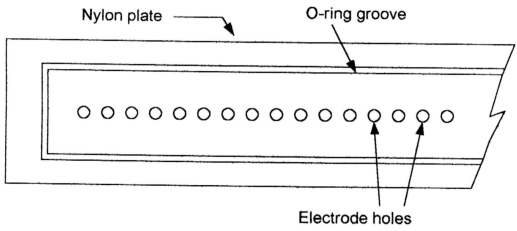

Figure 3.5 : Design of the nylon plate to hold and isolate 64 individual electrodes.

There are altogether sixty- four 3 mm diameter electrode holes along the nylon plate. Each electrode is connected to one separated capacitor. These electrodes are then plugged into these 3 mm electrode holes. These electrodes are thus electrically isolated from each other. However, this system does not achieve very high vacuum since each of these holes may cause a small leakage. Therefore, o-rings have been employed to hold vacuum at each electrode.

Since the whole channel comprises of three major parts, suitable o-rings play important roles in achieving good vacuum when these parts are screwed together.

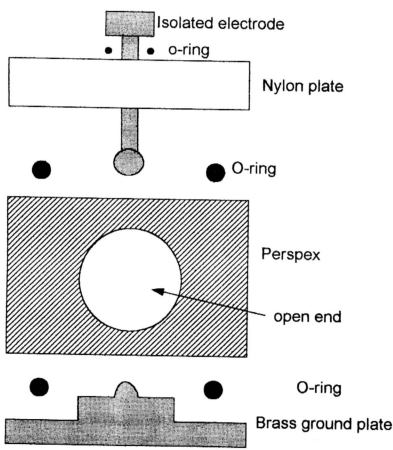

Figure 3.6 : Diagrammatic representation of the laser channel cross section.

Figure 3.6 shows how various parts of the laser channel are assembled. Two open holes at the end of the perspex channel will allow emission of the laser beam. A back mirror and quartz plate has been put at both the open ends. This will create an optical cavity for the laser. Besides, this mirror and quartz plate can also act as the vacuum flanges for both open ends of the channel.

In order to study the effects of different electrode profiles for the discharge, three different electrode profiles have been investigated. These pieces are then screwed to the M3 screw electrodes. In this experiment, three types of electrode profiles have been tested. The first profile is the sharp end screw itself. The second is a flat cylinder electrode profile and the third is a cylindrical electrode screwed on its side. The different electrode profiles are shown in Figure 3.7.

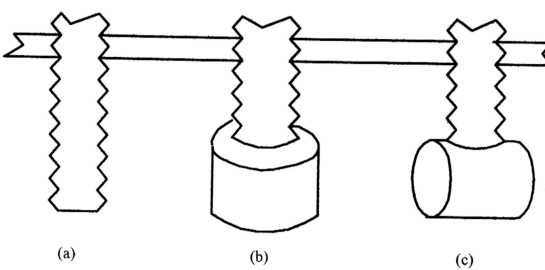

Figure 3.7 : Three electrode profiles. (a) The screw as an electrode. (b) The flat cylinder electrode profile. (c) The cylindrical electrode profile on its side.

The other side of the electrodes is a long copper rod welded on a brass plate which serves as the common electrode. The isolated electrodes are thus located only

at one side. Figure 3.8 shows the cross section view of the laser channel. When the laser channel breakdown, discharge occurs across the gap. The plasma formed will be constrained in cylindrical shape. These can be seen by the burn marks on the copper rod after a few discharges. Since the plasma is formed only between the isolated electrode and the copper rod, there are gaps between each isolated electrode. Although the plasma formed may be slightly expanded, the gap between the arcs is more or less 2 mm large apart as seen from the burn marks on the copper rod electrode.

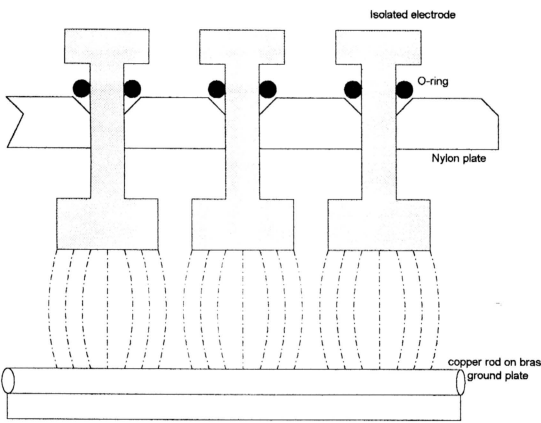

Figure 3.8 : The cross section of the isolated electrodes and the groundside of the transverse discharge laser.

Figure 3.8 also shows the discharge of laser channel. Laser beam comes out transversely with the discharge. Amplification occurs along the channel through each discharge. Although nitrogen laser is a super radiant laser, when a back mirror is put at one end, higher output will be obtained. The laser emits UV radiation, therefore, quartz plate has to be used as window instead of other materials because quartz will have minimum attenuation of UV radiation.

3.4 : Vacuum System

An Edward rotary pump is used to obtain vacuum inside the channel. An Edward CGS 125 mBar diaphragm gauge has been used as the gauge for the system. The piping for vacuum and gas flow is shown in Figure 3.9.

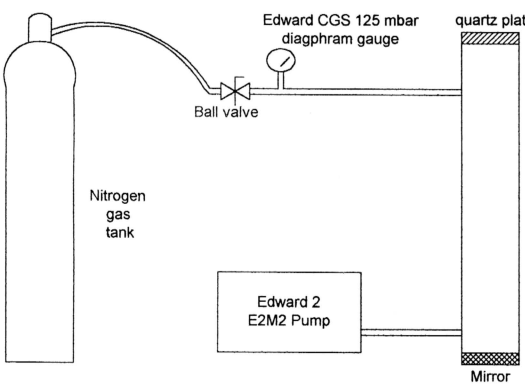

Figure 3.9 : Vacuum piping and the control valve of the gas flow for the laser system.

Nitrogen gas (OFN) is used as the medium for the discharge. Nitrogen gas is allowed to flow continuously into the channel and is pumped out through one outlet. A Swaglock ball valve has been employed to control the flow rate of nitrogen gas into the laser channel.

Good vacuum in the channel is very important because any impurity of the gas will affect the discharge and thus the optical output energy. Leakage may come from the 64 electrode holes. Some precautions have been taken to prevent small leakage. Vacuum grease has been put on every o-ring used in assembling the laser channel.

This system can hold a vacuum of 2 mbar. As the operation of the laser is around several tens of mbar, this small leakage is still acceptable.

3.5 : The high voltage supply

A 40 kV charger has been assembled for this project. The schematic drawing of the whole circuit is shown in Fig. 3.10.

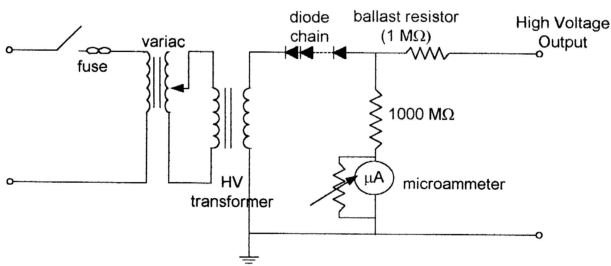

Figure 3.10 : Schematic drawing of high voltage supply circuit.

There are switches and fuse included in the charger for safety purposes. A 13A fuse is connected at the primary of the transformer while a variac is used to control the input voltage. The high voltage transformer is used to step up the voltage from a few hundred volts to several kilovolts. A diode chain consisting of a series of IN 4007 diodes has been used as rectifiers at secondary the output of the transformer. The charger is half-wave rectified. Polarity of diode chain is connected in such a way that the charger supplies negative high voltage to the system. It is found that the isolated electrodes must act as the cathode in order to have good discharge of every discrete electrode. Therefore, the charger is built with a negative charging voltage.

A 1MΩ resistor is connected in series with the diode chain to act as ballast resistor. This ballast resistor has the function of limiting the current flow to 40μA in the circuit. A voltmeter is connected across the circuit to show the charging voltage. This voltmeter is made up of a series of resistors with total resistance 1000MΩ connected in series with a micro-ammeter together with some potential meter. This will convert the micro-ammeter to a high voltage voltmeter after appropriate calibration.

3.6 : Pulsed Charging Circuit

A conventional "C-to-C" pulsing circuit has been employed in this experiment. The storage capacitor is a 0.1 μF Maxwell 31350 high voltage capacitor (100kV rating). Murata N4700 2nF doorknob capacitors and Matroc 5nF doorknob capacitors have been used as the peaking capacitors. Each of the peaking capacitors is connected to one of the isolated electrode. Insulated wires have been used to connect each separate peaking capacitor to each of the isolated electrodes. These wires are kept as close to the ground plate as possible. This will reduce the inductance of the discharge circuit as the cross section of the discharge loop is minimized. The actual setting and arrangement of the storage and peaking capacitors have been shown in Figure 3.2 and Figure 3.4. The equivalent circuit of the 'C-to-C' circuit is shown in Fig. 3.11.

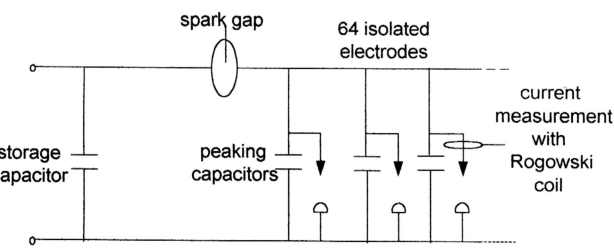

Figure 3.11 : Equivalent 'C-to-C' pulsing circuit used in the experiment.

A spark gap has been used as the switch for the "C-to-C" circuit. This spark gap is designed in such a way that the gap can be adjusted. In this experiment, the spark gap is adjusted so that it can hold up to 25 kV. Two gas inlets at the spark-gap also enable the spark-gap to be pressurized. It has been found that pressurized spark gap will reduce the jitter of the discharge in the spark gap. The design of the spark gap is as shown in Fig. 3.12.

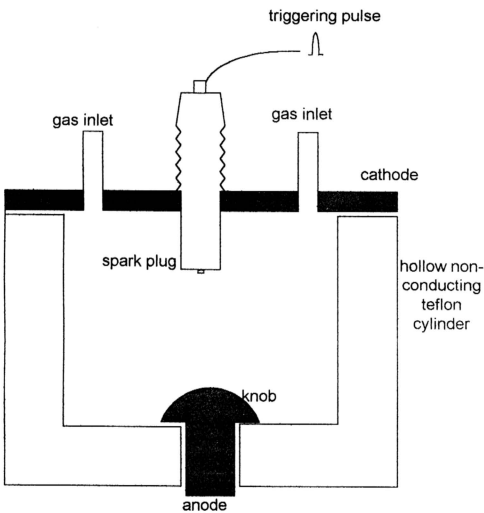

Figure 3.12 : Cross section view of the design of spark gap.

A triggering circuit is used to trigger the spark gap. This triggering unit is a standard SCR and UJT triggering unit. The UJT will generate continuous triggering for the circuit while the SCR generates the high voltage (~ hundreds of volt) trigger pulse. The electrical circuit is shown in Fig. 3.13.

The SCR generated voltage pulse is then sent to a car ignition coil. This car ignition coil will generate a very high peak voltage pulse to produce a spark at the spark plug in the spark gap. This spark will cause the spark gap to breakdown and thus switch on the high voltage.

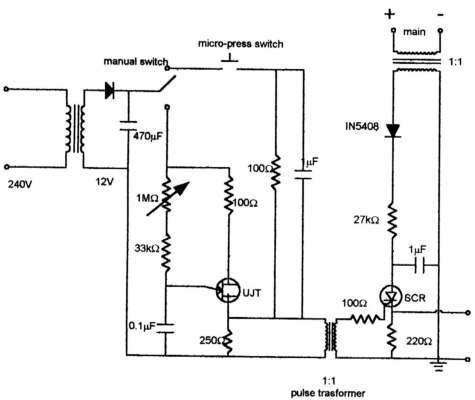

Figure 3.13 : Electrical Circuit of the UJT-SCR Triggering Unit

3.7 : Current Measurement

Rogowski coil is used to measure the current pulse of the discharge [33]. A Rogowski coil is a multi-turn solenoid, which has been coiled into a torus shape. The current to be measured is allowed to flow through the center of the torus as shown in Fig. 3.14.

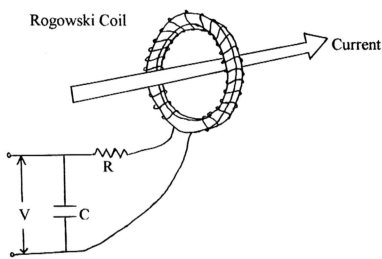

Figure 3.14 : The measurement of current using a Rogowski coil with passive integration network

Rogowski coil has the advantage that the magnetic field signals that is coupled to the coil is independent of the orientation in which the current passes through. However, it is found that the Rogowski coil cannot be too close or touching the current path. If not, distorted current signal will appear at the oscilloscope.

The voltage induced from the Rogowski coil is given by,

$$V = \mu \frac{NA}{S} \frac{dI}{dt}$$

$$I = \frac{S}{\mu_0 NA} \int V dt$$

where I = current

S = circumference of the major loop

μ_0 = permeability of free space

N = number of minor turns

A = cross section of the minor turn

Therefore, a RC integrator is needed in order to measure the current. A passive RC integrator is built with a 50 Ω terminator and is connected to the oscilloscope. A Tektronix TDS 360 oscilloscope and P6015A high voltage probe are used for the whole experiment. The equivalent circuit for the Rogowski coil and RC integrator is as shown in Fig. 3.15.

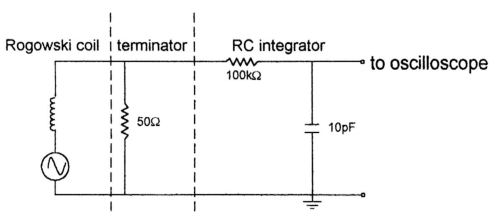

Figure 3.15 : Equivalent circuit from Rogowski coil through terminator and RC integrator.

Calibration of the Rogowski coil has been carried out. A simple LC discharge circuit is setup (as shown in Figure 3.16). The voltage waveform and the current waveform are measured and are recorded by the oscilloscope. The Rogowski coil is put at the return path of the circuit. This will reduce pick up of noise of the signal.

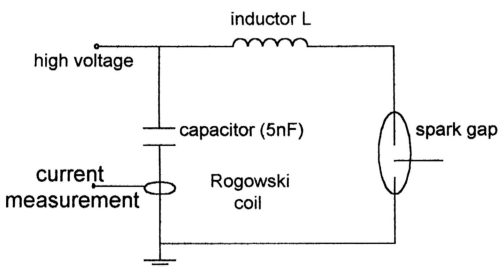

Figure 3.16 : LC circuit used to calibrate the Rogowski coil.

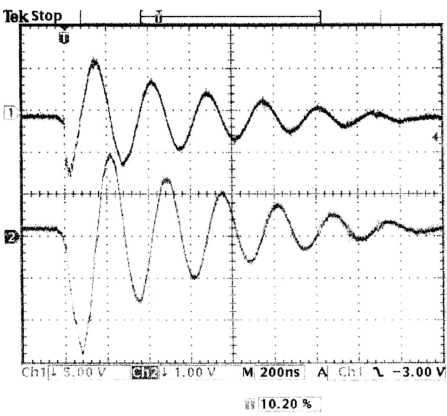

Figure 3.17 : CH1 is the voltage waveform across capacitor and CH2 is current waveform measured with Rogowski coil.

Figure 3.17 shows the voltage waveform and current waveform measured from the LC circuit for calibration purpose. From the sinusoidal waveform, the Rogowski coil can be calibrated with the approximate equation,

$$I = \frac{\pi C V_0 (1+f)}{T}$$

where C = capacitance of the LC circuit

V_0 = charging voltage of the LC discharge circuit

f = ratio of connective peaks of the sinusoidal current waveform

T = period of the oscillation waveform

From the measurement using the Rogowski coil with the proper RC integrator, it is found that the Rogowski coil gives a calibration factor of 0.85±0.01kA/V.

It is also found that the resistor for the RC integrator should be larger than the capacitance in order to get a clean signal. Copper tape has been used to wrap the whole coil and is connected to the ground of the circuit because in a pulse system, the rapidly varying magnetic field, B, will cause the coil to pickup spurious signals. This layer of copper will act as the shield of the coil from RF noise and other EM noise. The shielding layer does not cover the coil completely. A thin opening inside the torus will allow the coil to pick up the current signal as shown in Figure 3.18. Moreover, the shield layer must be thick enough to perform better shielding. The slotted shielding layer prevents the electrostatic noise from disturbing the signal pickup.

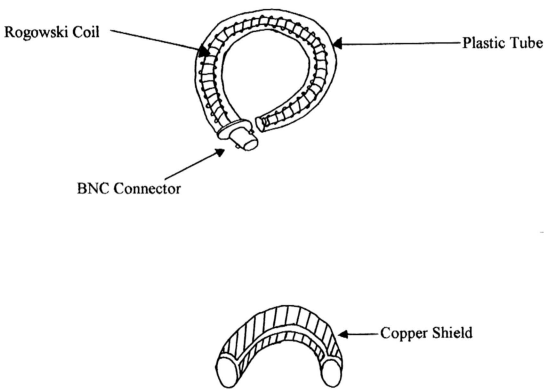

Figure 3.18 : The insulation shielding layer and noise shielding layer for Rogowski coil. A small slit opening at inner side of the torus.

3.8 : Output Energy and optical pulse diagnostic

Ophir Model PE-19 pyrodetector and Ophir Nova Display 26777 joulemeter have been used to measure the output energy of the laser. The diagram of the setup of photodiode is shown in Figure 3.19.

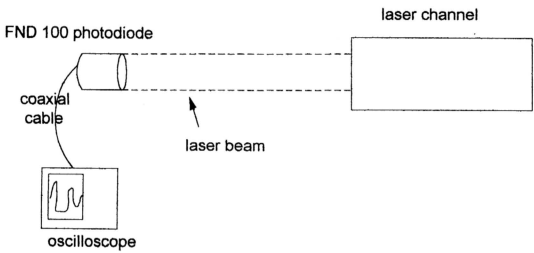

Figure 3.19 : Setup for optical pulse measurement.

An EG&G FND 100 photodiode (1ns rise time) is used to detect the optical pulse. Operating at photoconductive mode, the photodiode is reverse biased with a 90V battery. The equivalent circuit is shown in Fig. 3.20.

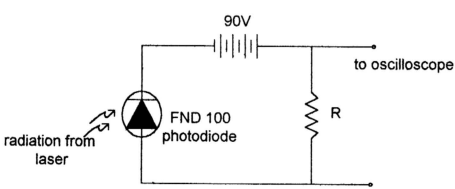

Figure 3.20 : Equivalent circuit for photodiode and optical pulse detection.

A 2m long coaxial cable with 50Ω terminator is used to send the signal from the photodiode to the oscilloscope. A similar coaxial cable is used to connect the Rogowski coil to the oscilloscope in the previous experiment. The signal is observed from the oscilloscope. The optical pulse is saved and the pulse width is measured.

3.9 : Measurement of the wavelength of the optical output

The wavelength of the optical output is measured by utilizing a PTI spectrometer with 1200 g/mm diffraction grating. The optical pulse is directed into the spectrometer as shown in Figure 3.21. The optical output radiated from the laser goes into the spectrometer through the input aperture of the spectrometer. The grating in the spectrometer will diffract the optical pulse into certain angle according to the wavelength of the optical pulse. The wavelength measured from this experiment is 337.1nm. Such UV line for nitrogen gas is the transition at the second positive band of the nitrogen molecule.

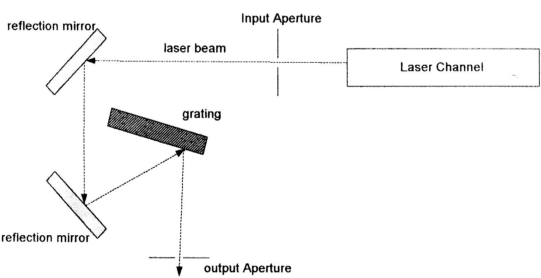

Figure 3.21 : Setup of the experiment of measuring the laser output wavelength.

3.10 : Measurement of output energy with various number of electrodes

The gain of each arc is of interest in this experiment. A small piece of thick mylar sheet is cut and put into the discharge channel. This mylar sheet will act as a optical barrier that limits the number of arcs contributing to the laser output. Figure 3.21 shows the schematic drawing of the setup of the experiment. The output energy of the laser is recorded and a graph is plotted.

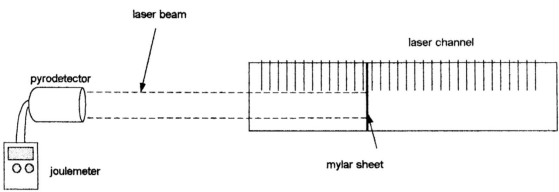

Figure 3.22 : Setup of the experiment of investigating the contribution of the number of arcs to laser action.